

This article is licensed under a Creative Commons Attribution-NonCommercial NoDerivatives 4.0 International License.

Corosolic Acid Inhibits Cancer Progress Through Inactivating YAP in Hepatocellular Carcinoma

Ming Jia,*¹ Yulin Xiong,^{†1} Maoshi Li,* and Qing Mao*

*Institute of Infectious Diseases of Chinese PLA, Southwest Hospital, Third Military Medical University (Army Medical University), Chongqing, P.R. China

[†]Department of Laboratory, The Fourth Medical Center of PLA General Hospital, Beijing, P.R. China

Chemotherapy is critical for the treatment of hepatocellular carcinoma (HCC). Despite the proapoptotic effects of corosolic acid (CA) treatment, its underlying mechanism is not completely clear. The aim of this study was to determine the molecular mechanism of CA in HCC treatment. MTT assay was used to determine the IC₅₀ of CA. Immunoprecipitation and immunofluorescence were used to detect the interaction and subcellular localization of Yes-associated protein (YAP) and mouse double minute 2 (MDM2). In addition, *in vivo* xenotransplantation was performed to assess the effects of CA, YAP, and MDM2 on tumorigenesis. The IC₅₀ of CA was about 40 μM in different HCC cell lines, and CA decreased YAP expression by reducing its stability and increasing its ubiquitination. CA treatment and MDM2 overexpression significantly decreased the cross-talk between YAP and cAMP-responsive element-binding protein (CREB), TEA domain transcription factor (TEAD), and Runt-related transcription factor 2 (Runx2). CA stimulation promoted the translocation of YAP and MDM2 from the nucleus to the cytoplasm and increased their binding. In addition, CA treatment obviously reduced tumorigenesis, whereas this effect was abolished when cells were transfected with sh-MDM2 or Vector-YAP. The present study uncovered that CA induced cancer progress repression through translocating YAP from the nucleus in HCC, which might provide a new therapeutic target for HCC.

Key words: Hepatocellular carcinoma (HCC); Corosolic acid (CA); Yes-associated protein (YAP); Mouse double minute 2 (MDM2)

INTRODUCTION

Hepatocellular carcinoma (HCC) is the fifth most common cancer in the world¹. It is currently the second leading cause of cancer-related deaths, accounting for approximately 800,000 deaths every year². In general, the clinical treatments for HCC include surgery, chemotherapy, radiation, and liver transplantation. Among them, surgical resection of tumors and liver transplantation often have a curative effect in patients³. However, owing to poor prognoses and high recurrence rates after resection, a large number of patients present with advanced disease and are not eligible for surgery^{4,5}. Although chemotherapy is an alternative choice for advanced HCC, the efficacy of chemotherapy is often hampered by a range of adverse side effects that cause patient suffering and even death⁶. Therefore, it is urgent to focus on the development of more effective therapeutic drugs against HCC with fewer side effects.

In recent years, Chinese herbal medicines have been extensively used in various anticancer studies, and a number of them have been shown to have anticancer properties⁷⁻⁹. Compared to Western medicine used at a certain stage of cancer treatment, Chinese herbal medicine always shows less toxicity and is a more efficient treatment, and tumor recurrence and metastasis are less likely⁸. Among these herbal medicines, *Actinidia valvata* Dunn (Actinidiaceae), a shrub that mainly grows in eastern China, has a series of applications in traditional Chinese medicine and as a folk herb. The root of this plant, commonly known as Mao renshen in China, exhibits notable anti-inflammatory and antitumor activities and has cytotoxic effects against several types of cancer cells, including liver cancer cells¹⁰. Corosolic acid (CA), which is found in water extracts of *Actinidia chinensis*, also exhibits significant anticancer effects in HCC cells by decreasing HCC cell migration without cytotoxicity¹¹.

¹These authors provided equal contribution to this work.

Address correspondence to Qing Mao, M.S., Institute of Infectious Diseases of Chinese PLA, Southwest Hospital, Third Military Medical University (Army Medical University), Gaotanyan Centre Street No. 30, Shapingba District, Chongqing 400038, P.R. China. E-mail: maoqing2020@126.com

However, the pharmacological activity of CA remains poorly understood.

Cancer cell proliferation is a critical process in tumor development^{12,13}; thus, antiproliferation therapy is an important approach for cancer treatment. The Hippo pathway plays a critical role in controlling organ size by regulating cell growth, proliferation, and apoptosis¹⁴⁻¹⁶. Emerging evidence has demonstrated that Yes-associated protein 1 (YAP), the downstream effector of the tumor suppressor Hippo pathway, serves as an oncoprotein that significantly contributes to liver tumorigenesis¹⁷. In addition, YAP acts as a central node that connects the cAMP-dependent protein kinase (PKA)/cAMP-responsive element-binding protein (CREB), mitogen-activated protein kinase kinase (MEK)/extracellular signal-regulated kinase (ERK), phosphatidylinositol 3-kinase (PI3K)/AKT, p70S6K/mammalian target of rapamycin (mTOR), and c-Jun/c-Fos signaling pathways and thereby forms a complex network that maintains transformative phenotypes in liver cancer cells¹⁸⁻²⁰, suggesting that molecules that inhibit YAP may be effective therapeutic targets in HCC.

In the present study, we aimed to clarify the relationship between CA and YAP and to reveal the mechanism of CA in the inhibition of HCC.

MATERIALS AND METHODS

Cell Culture Conditions

The HCC cell lines Hep3B and HepG2 were purchased from the American Type Culture Collection (ATCC; Manassas, VA, USA). SMMC-7721, Huh7, and HLE cells were purchased from the Cell Bank of the Chinese Academy of Sciences (Shanghai, China). Huh7 cells were cultured in Dulbecco's modified Eagle's medium (Gibco, Boston, MA, USA), Hep3B and HepG2 cells were cultured in Eagle's minimum essential medium, and SMMC-7721 and HLE cells were cultured in RPMI-1640 medium (Gibco). All the culture media were supplemented with 10% fetal bovine serum (FBS; Gibco), 100 µg/ml penicillin, and 100 µg/ml streptomycin. All cells were maintained in a humidified incubator with 5% CO₂ at 37°C. In all experiments, cells were allowed to adhere prior to their exposure to CA (formula: C₃₀H₄₈O₄; No. 4547-24-4, Sigma-Aldrich, St. Louis, MO, USA) at different concentrations (0, 10, 20, 40, 80, and 160 µM), with 0.1% dimethyl sulfoxide (DMSO) as control. Cells were treated with 10 µM MG132 (a proteasome inhibitor; Sigma-Aldrich) or 100 µg/ml cycloheximide (CHX; a protein synthesis inhibitor; Sigma-Aldrich) to assess the protein degradation manner. To determine the extent of apoptosis in our assays, we collected all fractions and attached and floating cells in the culture supernatant.

RNA Interference and Cell Transfection

A plasmid overexpressing mouse double minute 2 (MDM2) (vector-MDM2, No. SC118660) and its negative

control vector (vector-NC), as well as the overexpressing lentivirus vector used to upregulate YAP (vector-YAP), were all purchased from OriGene (Rockville, MD, USA). The short hairpin RNAs (shRNAs) used to downregulate human MDM2 (sh-MDM2) and YAP (sh-YAP) expression were obtained from GenePharma (Shanghai, China). Cells were transfected with vector-MDM2 and vector-NC using INTERFERin® transfection reagent (Polyplus, France) according to the manufacturer's instructions. In brief, a total of 2 × 10⁵ cells were transfected with 2 µg of DNA. The transfection efficiency was detected by Western blotting and real-time polymerase chain reaction (RT-PCR) after 48 or 24 h of transfection, respectively.

Western Blotting Analysis

Cells were extracted in lysis buffer containing 50 mM sodium chloride (NaCl), 1 mM ethylene glycol tetraacetic acid, 0.1% sodium dodecyl sulfate (SDS), 1 mM sodium fluoride, 1 mM sodium orthovanadate, 1 mg/ml aprotinin, 1 mg/ml leupeptin in 10 mM Tris buffer (pH 7.4), and proteinase inhibitor (1 mM phenylmethanesulfonyl fluoride). Equal amounts of total protein were separated on a 10% SDS-polyacrylamide gel and transferred to a nitrocellulose membrane (Millipore, Billerica, MA, USA). The membranes were incubated overnight with monoclonal antibodies against glyceraldehyde-3-phosphate dehydrogenase (GAPDH), cleaved caspase 3/9, caspase 3/9, TEA domain transcription factor (TEAD), CREB, Runx2, YAP, p-YAP, MDM2, p53, histone, and tubulin; all were purchased from Cell Signaling Technology (Danvers, MA, USA). The membrane was washed three times with Tris-buffered saline-Tween 20 (TBST) containing 24.2 g of Tris base, 80 g of NaCl, and 0.1% (v/v) Tween 20 for a total of 1 L. Next, the membranes were incubated with secondary antibodies (Biorworld, St. Louis Park, MN, USA) at 37°C for 1 h. The signals were visualized using a Luminata Crescendo Western horseradish peroxidase substrate (Millipore).

RNA Extraction and RT-PCR

Total RNA was extracted by TRIzol reagent (Invitrogen, Carlsbad, CA, USA). RT-PCR was performed to amplify the cDNA using primers specific for MDM2 mRNA (forward: 5'-ACGACAAAGAAAACGCCACA-3' and reverse: 5'-GTAACCTTGATATACACCAGCATCAA-3'), CTGF mRNA (forward: 5'-GTGGAGTATGTACCGACGGC-3' and reverse: 5'-GCAGGCACAGGTCTTGATGA-3'), ANKRD1 mRNA (forward: 5'-CCTGTGGATGTGCTACGTT-3' and reverse: 5'-ACAGGCGATAAGATGCTCCG-3'), and GAPDH mRNA (forward: 5'-ATCATCCCTGCCTCTACTGG-3' and reverse: 5'-GTCAGGTCCACCACTGACAC-3'). The RNA input was normalized to the level of GAPDH. All reactions were carried out using SYBR Green Mix (TaKaRa, Dalian, China).

RT-PCR was carried out using an ABI 7500 real-time PCR system (Invitrogen). RT-PCR data were analyzed by the $2^{-\Delta\Delta Ct}$ method²¹.

Cytoplasmic and Nuclear Fractionation

Cytoplasm and nuclear fractionation were performed according to the manufacturer's instructions (Thermo Fisher Scientific, Waltham, MA, USA). In brief, cells were harvested and washed once with cold phosphate-buffered saline (PBS) (pH 7.4) containing 19 g of NaCl, 0.3 g of $\text{Na}_2\text{HPO}_4 \cdot 2\text{H}_2\text{O}$, and 6 g of $\text{Na}_2\text{HPO}_4 \cdot 12\text{H}_2\text{O}$ for a total of 1 L. The cells were then lysed with the help of NE-PER Nuclear & Cytoplasmic extraction kit (Thermo Fisher Scientific) according to the manufacturer's protocol. The cytoplasmic and nuclear fractionation samples were stored at -80°C in preparation for Western blotting detection.

Immunoprecipitation

To carry out immunoprecipitation (IP), HepG2 cells were treated with 0.1% DMSO (control) or CA for 24 h and lysed in lysis buffer containing 50 mM NaCl, 1 mM ethylene glycol tetraacetic acid, 0.1% SDS, 1 mM sodium fluoride, 1 mM sodium orthovanadate, 1 mg/ml aprotinin, 1 mg/ml leupeptin in 10 mM Tris buffer (pH 7.4), and 1 mM phenylmethanesulfonyl fluoride. The lysates were then sonicated and centrifuged, and the supernatant was incubated with anti-YAP antibody (Cell Signaling Technology) overnight at 4°C . The immunocomplexes were then incubated with PureProteome magnetic beads (Millipore) for 1 h at 4°C , washed, eluted with protein sample buffer (Millipore), and analyzed by Western blotting.

Cell Viability Assay

Cell viability was determined by measuring the absorbance of 3-(4,5-dimethylthiazol-2-yl)-2,5-diphenyltetrazolium bromide (MTT) dye after staining the living cells. Briefly, cells were incubated in 100 μl of media in 96-well plates at an initial cell density of 1×10^6 cells/ml. After 24 h of incubation, different concentrations of CA were added to the cells, and an appropriate volume of drug vehicle was added to untreated cells. After 0, 24, 48, 72, and 96 h of incubation, 10 μl of an MTT solution (5 mg/ml in PBS) was added, and the cells were incubated for an additional 3 h. An SDS/isobutanol/HCl solution (100 μl) (10% SDS, 5% isobutanol, and 12 μM HCl) was added to each culture and incubated overnight. Relative cell viability was determined by scanning with a microplate reader (Bio-Rad, San Diego, CA, USA) with a 570-nm filter. Cells in five wells per dose were counted in each experiment.

Colony Formation Assay

HepG2 cells transfected with sh-MDM2, vector-YAP, or the control vectors were collected and seeded on a

6-cm dish at a density of 200 cells for each well. Cells were continually treated with 40 μM CA. Following incubation at 37°C for 14 days, the cells were stained with 0.1% crystal violet for 20 min and were washed with PBS three times.

Flow Cytometry Analysis

HepG2 cells were seeded into a 6-cm plate and given different treatments. Following 48 h of incubation at 37°C , annexin V-fluorescein isothiocyanate (FITC)/propidium iodide (PI) (BD Biosciences, San Diego, CA, USA) was added into the cell suspension and incubated for 5 min in the dark. Cell apoptosis was detected by using a flow cytometer (BD FACSCanto II, BD Biosciences) and analyzed using FlowJo 7.6 software.

Immunofluorescence Staining

HepG2 cells at 10% confluence were seeded onto small glass coverslips and placed into 24-well plates. After 24 h of culture, CA (40 μM) was applied. The coverslips were then removed, washed with PBS three times, fixed with 100% methanol (-20°C) for 15 min at room temperature, washed with PBST three times, and blocked for 1 h with 5% goat serum in PBS. Next, the cells were incubated with anti-Runx2 (1:1,000 dilution; No. #12556; Cell Signaling Technology), anti-CREB (1:500 dilution; No. #9197; Cell Signaling Technology), or anti-TEAD (1:150 dilution; No. ab221367; Abcam, Cambridge, MA, USA) antibodies overnight at 4°C and then incubated with immunoglobulin G (IgG) AF568 (red; Life Technologies, Carlsbad, CA, USA) or IgG AF488 (green; Life Technologies) at room temperature in the dark for 1 h. Finally, the cells were treated with 4',6-diamidino-2-phenylindole (DAPI) ($1:1 \times 10^4$) for 5 min, followed by being washed three times with PBST and covered with antifade mounting medium (Vectashield, Loerrach, Germany) and placed onto microscope slides. The slides were examined under a laser scanning microscope (TCS-SP2-AOBS-MP; Leica Microsystems CMS, Wetzlar, Germany).

Tumorigenicity Assays in Nude Mice

This study was carried out in strict accordance with the recommendations of the National Institutes of Health *Guide for the Care and Use of Laboratory Animals*. The protocol was approved by the Committee on the Ethics of Animal Experiments of Southwest Hospital, Third Military Medical University (Army Medical University). All surgeries were performed under sodium pentobarbital anesthesia, and all efforts were made to minimize suffering. Six-week-old female nude mice weighing 20–22 g were subcutaneously injected in the right armpit region with 1×10^7 cells in 0.1 ml of PBS. After xenografts were visible (10 days after injection), the mice were treated with CA (10 mg/kg) for another 28 days before the tumor

sizes were measured, and equal DMSO was used as a negative control. Four groups of mice ($n = 6/\text{group}$) were tested. Group 1 (control) mice were injected with HepG2 cells infected with negative control (vector-NC and sh-NC) and treated with DMSO; group 2 mice (CA) were injected with HepG2 cells infected with negative control and treated with CA; group 3 mice (CA + vector-YAP) were injected with HepG2 cells infected with vector-YAP and treated with CA, and group 4 (CA + sh-MDM2) mice were injected with HepG2 cells infected with shRNA-MDM2 and treated with CA.

Statistical Analysis

All data were analyzed by SPSS 23.0 statistical software (SPSS Inc., Chicago, IL, USA) and are expressed as the mean \pm standard deviation (SD). The significance of the differences between the means of the treated and untreated groups was compared by one-way analysis of variance (ANOVA) followed by unpaired Student's *t*-test, and a value of $p < 0.05$ indicated statistical significance.

RESULTS

Determination of the IC_{50} Value of CA

To determine the IC_{50} value of CA, we treated SMMC-7721, Hep3B, HepG2, Huh7, and HLE cells with serial concentrations (0, 10, 20, 40, 80, and 160 μM) of CA. Figure 1A showed the chemical structure of CA. The IC_{50} of CA in SMMC-7721, Hep3B, HepG2, Huh7, and HLE were 41.2, 40.2, 40.5, 40, and 41.3 μM , respectively (Fig. 1B–F). In addition, 40 μM CA treatment induced significant increases in the levels of cleaved caspase 3/caspase 3 and cleaved caspase 9/caspase 9 (Fig. 1G–K). Therefore, we chose 40 μM CA for the next experiments.

CA Treatment Reduces YAP Expression and Stability

We next explored the underlying mechanism of CA in the progression of HCC. YAP expression was significantly reduced, while its phosphorylation level (p-YAP) was increased when HepG2, Huh7, and Hep3B cells were treated with 40 μM CA for 24 h compared to the control group (Fig. 2A–C). Next, we evaluated how CA regulated YAP expression in HCC cells. CA treatment significantly enhanced the ubiquitination of YAP protein compared to that of the control group (Fig. 2D). Furthermore, we found that treatment with CA in HepG2 cells shortened the half-life of YAP compared to that measured in the control group (Fig. 2E). Together, these results suggested that stimulation with CA inhibited YAP activation.

CA Treatment Translocates YAP From the Nucleus to the Cytoplasm

As shown in Figure 3A, CA treatment translocated YAP protein from the nucleus to the cytoplasm. As the pro-oncogenic role of YAP is controlled by its transcription

target, such as CREB, Runx2, and TEAD, we tested whether CA controls YAP via modulating the binding of YAP to CREB, Runx2, and TEAD. Treatment with CA triggered YAP protein from the nucleus to the cytoplasm and reduced its binding to CREB, Runx2, and TEAD, as shown by the immunofluorescence (Fig. 3B–D) and IP results (Fig. 3E). These results indicated that stimulation with CA inhibited HCC development through inactivating YAP signaling.

A previous study reported that YAP bound to MDM2 (an E3 ubiquitin ligase) to induce the ubiquitination and degradation of 14-3-3 ζ ²². Accordingly, we explored the effect of MDM2 on CA-induced YAP ubiquitination. Compared with the control group, CA treatment significantly increased the expression of MDM2 protein, with no obvious influence in p53 expression in HepG2, Huh7, and p53-null Hep3B cells (Fig. 4A–C). We then explored MDM2 roles in the interactions between YAP and CREB, Runx2, and TEAD proteins in HepG2 cells. The expression of MDM2 was significantly elevated when HepG2 cells were transfected with vector-MDM2, as detected by RT-PCR and Western blotting assays (Fig. 4D). The IP result demonstrated that MDM2 overexpression significantly weakened the binding of YAP protein to CREB, Runx2, and TEAD in HepG2 cells (Fig. 4E). Furthermore, compared with the control group, the expressions of CTGF and ANKRD1, downstream genes of YAP signaling, were also decreased when cells were transfected with vector-MDM2 (Fig. 4F). These data illustrated that stimulation with CA decreased YAP expression via increasing MDM2 in HCC cells.

CA Treatment Enhances the Interaction Between YAP and MDM2

We then further revealed the role of MDM2 in stimulation with CA-induced YAP expression decrease. The expression level of MDM2, which bound to YAP protein, was increased when HepG2 cells were treated with CA in a dose-dependent manner (Fig. 5A). Compared with the control group, CA treatment significantly increased the contents of MDM2 and YAP in cytoplasm, while reducing their expression levels in nuclear, as determined by Western blotting (Fig. 5B–D) and immunofluorescence technology (Fig. 5E). In addition, we explored the role of MDM2 in CA-induced nuclear exportation of YAP protein. MDM2 expression was significantly decreased when HepG2 cells were transfected with sh-MDM2 compared with the sh-NC group (Fig. 5F). Knockdown of MDM2 increased YAP expression and decreased its ubiquitination (Fig. 5G). Moreover, downregulation of MDM2 significantly abolished CA's role in the translocation of YAP protein from the cytoplasm to the nucleus (Fig. 5H and I). These results suggested that CA treatment inhibited the activation of YAP in a MDM2-dependent manner.

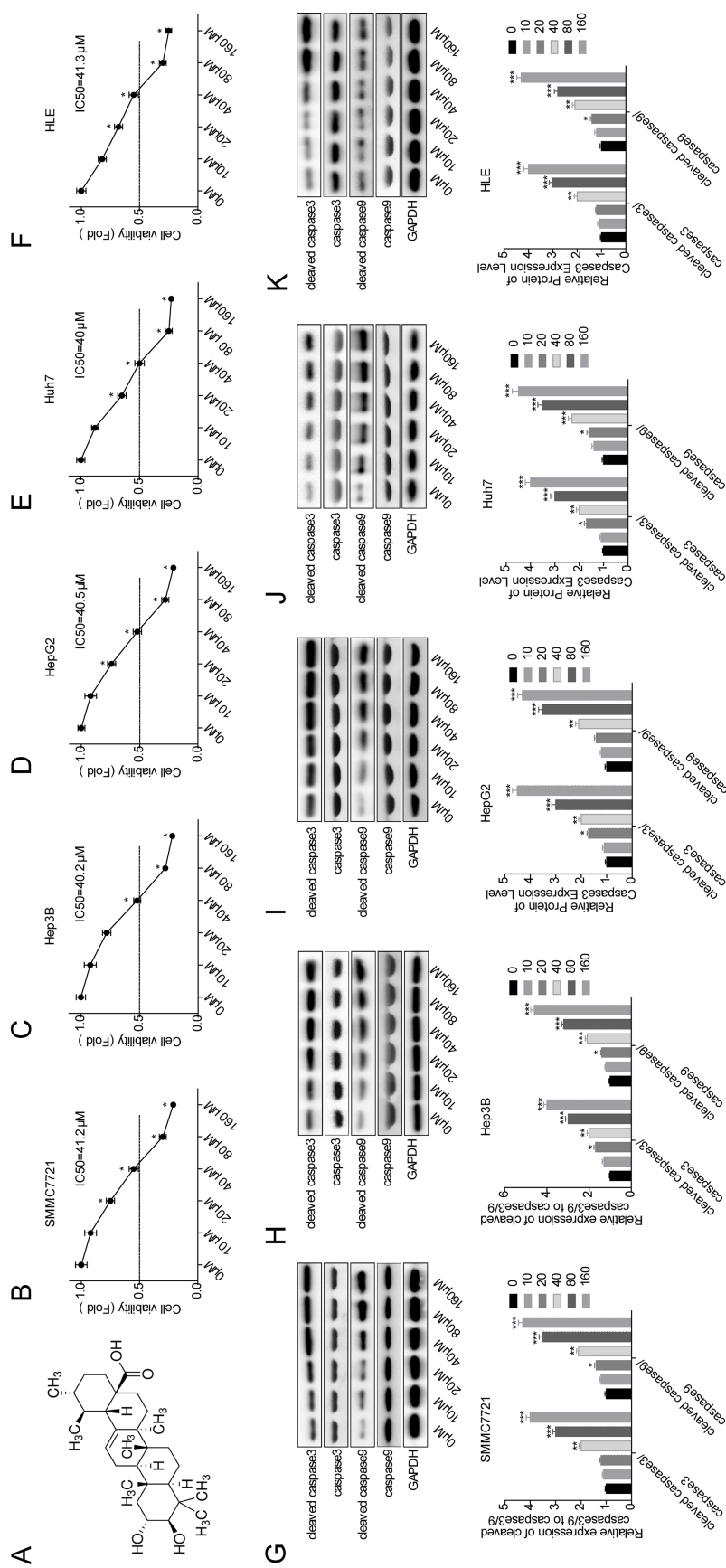


Figure 1. Determination of the IC₅₀ value of corosolic acid (CA). (A) The chemical structure of CA. (B-F) Cytotoxicity induced by CA administration (0, 10, 20, 40, 80, and 160 μM, 24 h) was measured by MTT assay in SMMC-7721, Hep3B, HepG2, Huh7, and HLE cells. (G-K) Western blotting analysis was carried out using anticaspase 3/9 antibodies in SMMC-7721, Hep3B, HepG2, Huh7, and HLE cells treated with the indicated concentrations of CA for 24 h. The relative cleaved caspase 3/9 levels were normalized to those of caspase 3/9, and the levels from cells without CA treatment (0 μM) were arbitrarily set to “1.” **p* < 0.05, ***p* < 0.01, ****p* < 0.001.

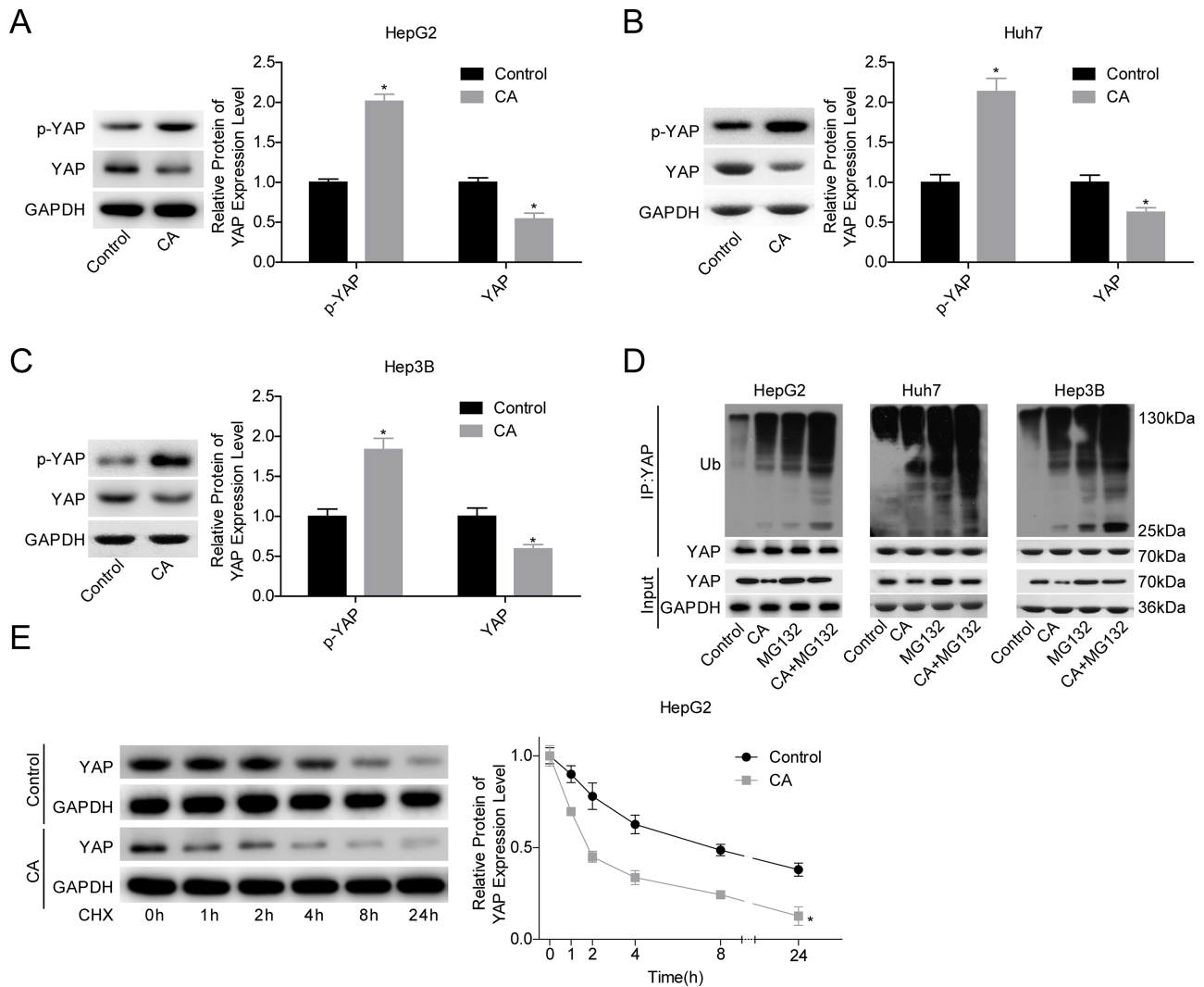


Figure 2. Evaluation of the effect of CA on Yes-associated protein (YAP). (A–C) Western blotting analysis of the effects of CA (40 μ M) on the expressions of YAP and p-YAP in the HepG2, Huh7, and Hep3B cell lines. (D) Immunoprecipitation (IP) assay analysis of the ubiquitination of YAP after HepG2, Huh7, and Hep3B cells were treated with CA (40 μ M). (E) Cycloheximide (CHX) chase experiments of YAP in HepG2 cells treated with the same amount of dimethyl sulfoxide (DMSO) or CA (final concentration of 40 μ M) for the indicated times. Representative Western blots are shown. The relative expression levels of YAP were normalized to those of glyceraldehyde-3-phosphate dehydrogenase (GAPDH). * $p < 0.05$.

CA Treatment Repressed the Progression of HCC via Modulating the MDM2/YAP Axis

Finally, we investigated the effect of the MDM2/YAP axis in CA-induced inhibition of HCC progression. Cell transfection with vector-YAP or sh-MDM2 significantly impaired CA-induced YAP expression repression (Fig. 6A). Moreover, the inhibitions of cell colony formation (Fig. 6B) and proliferation (Fig. 6C) induced by CA treatment were obviously neutralized when HepG2 cells were transfected with sh-vector-YAP or sh-MDM2, as well as the promotion of cell apoptosis induced by CA (Fig. 6D). Furthermore, CA administration significantly reduced in vivo tumor growth, whereas this effect was significantly

impaired when cells were transfected with vector-YAP or sh-MDM2 (Fig. 6E–G). The above results illustrated that CA treatment repressed HCC progression via downregulating YAP expression and upregulating MDM2 expression.

DISCUSSION

The use of Chinese herbal medicine in cancer treatment, either alone or in conjunction with Western medicine, shows much promise in both the laboratory and the clinic⁸. A previous study¹¹ indicated that CA displayed anticancer activities in vitro and in vivo in the treatment of HCC cells. Specifically, CA stimulation exhibited anti-migratory activity and antitumor effects in a xenograft

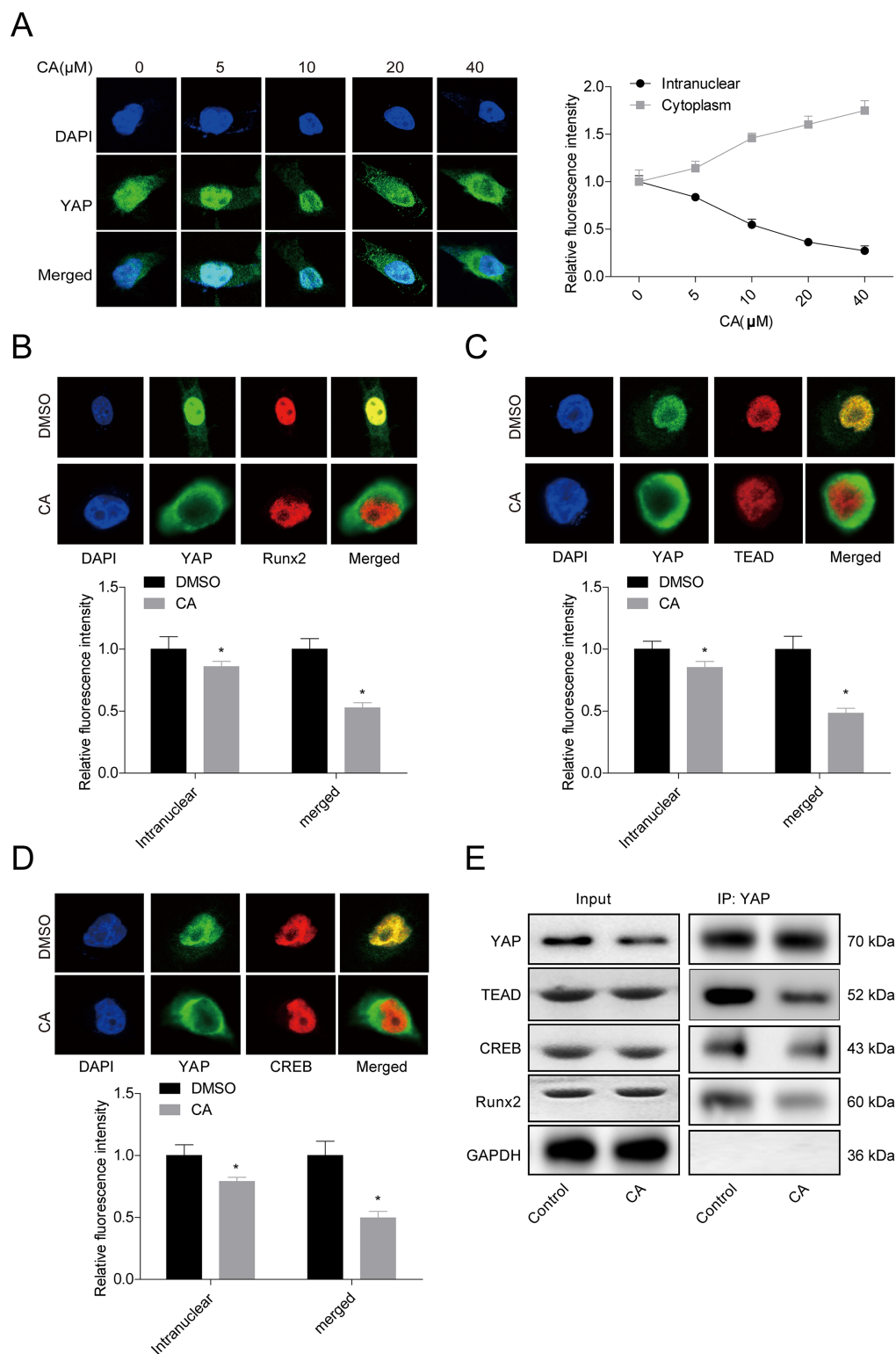


Figure 3. The effect of CA treatment on the intracellular localization of YAP and its interaction with cAMP-responsive element-binding protein (CREB), TEA domain transcription factor (TEAD), and Runx2. (A) CA treatment affected the intracellular localization of YAP, as measured by the immunofluorescence in HepG2 cells treated with different concentrations of CA. (B–D) CA treatment affected the binding of YAP to CREB, TEAD, and Runx2, as measured by the immunofluorescence in HepG2 cells treated with 40 μM CA. Representative immunofluorescence images are shown. * $p < 0.05$. (E) CA treatment affected the binding of YAP to CREB, TEAD, and RUNX2, as measured by IP in HepG2 cells treated with 40 μM CA.

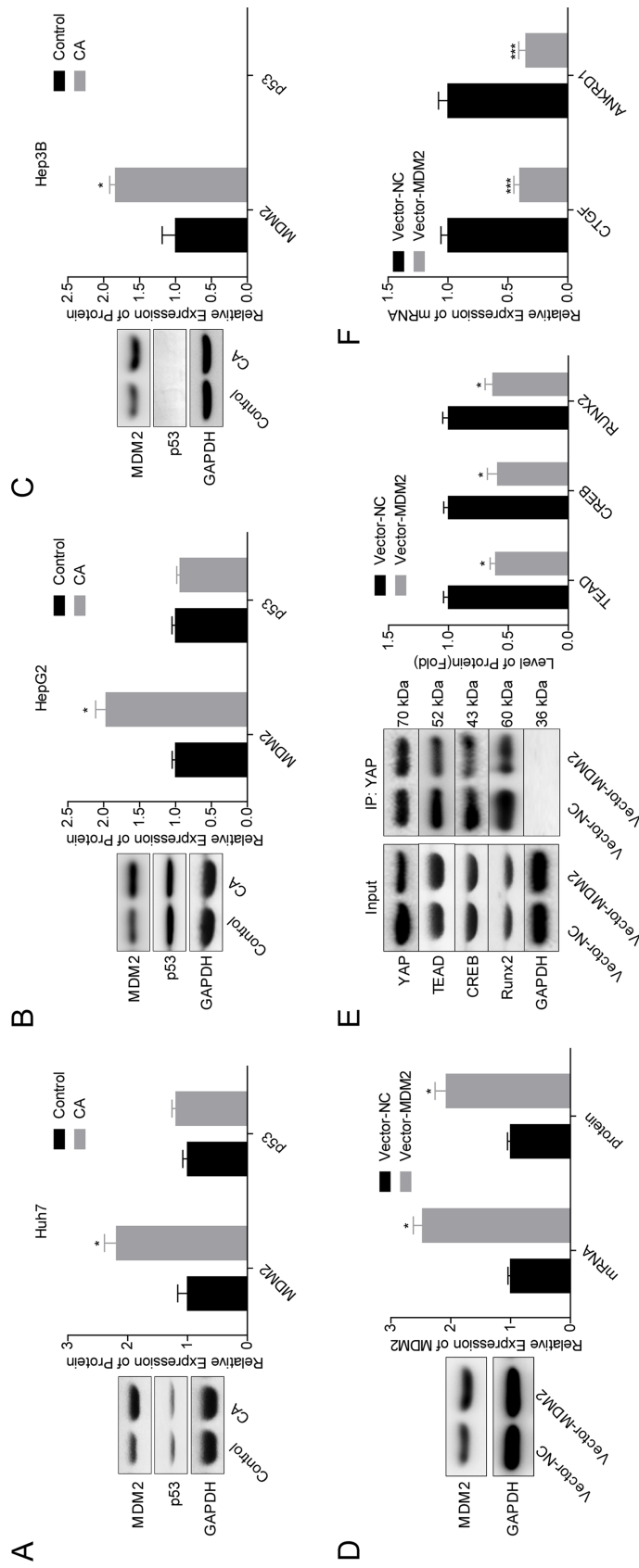


Figure 4. The effects of MDM2 on the expression of genes related to YAP signaling. (A–C) The expression levels of MDM2 and p53 were determined by Western blotting after HepG2, Huh7, and Hep3B cells were treated with 40 μ M CA for 24 h. (D) Western blotting and real-time polymerase chain reaction (RT-PCR) analysis of the transfection efficiency of vector-mouse double minute 2 (MDM2). (E) IP analysis of the interaction between YAP and CREB, TEAD, or RUNX2 induced by vector-MDM2. (F) RT-PCR analysis was used to detect the expression of CTGF and ANKRD1 in HepG2 cells with different treatments. * $p < 0.05$, *** $p < 0.001$.

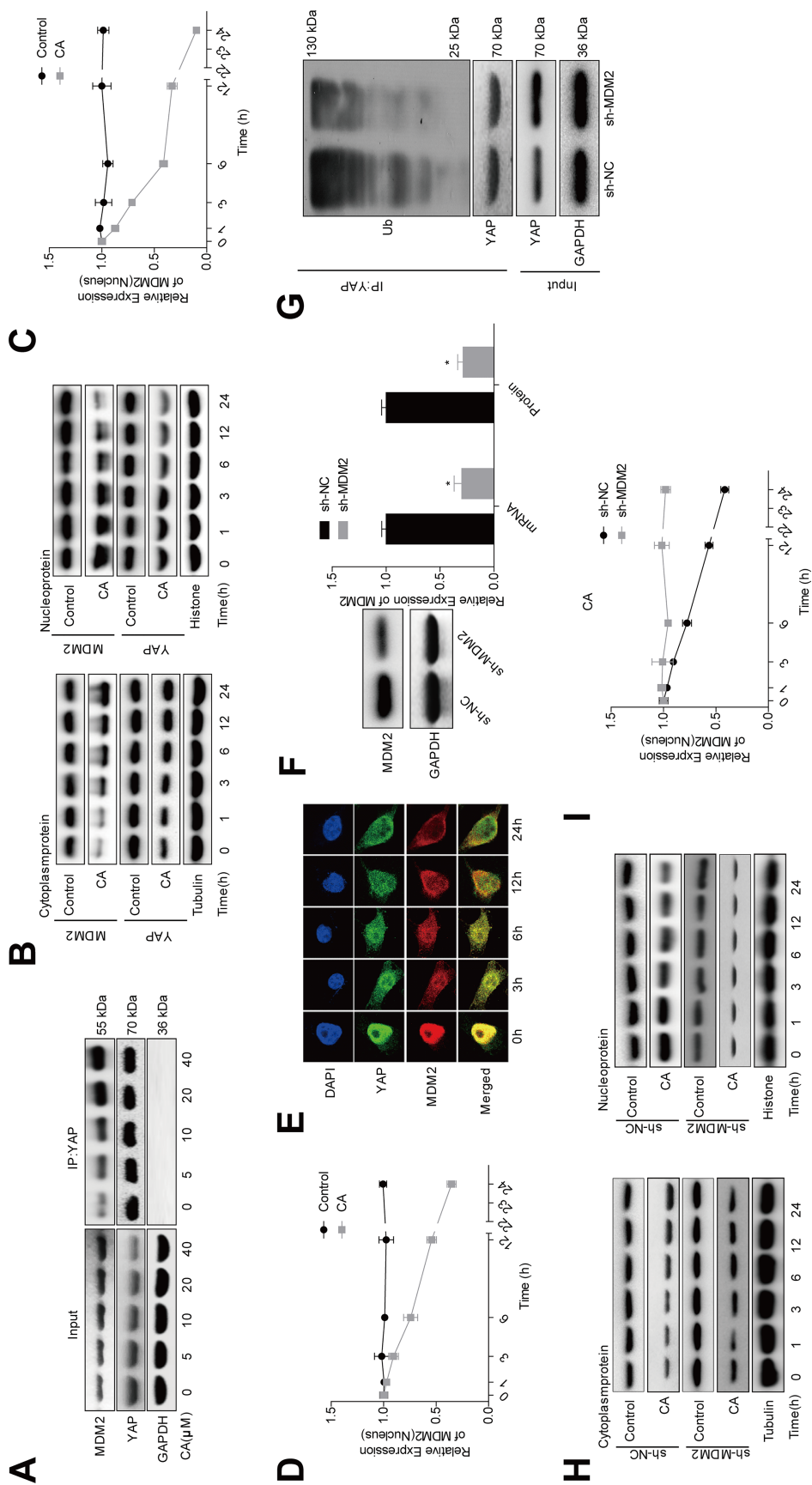


Figure 5. The effects of MDM2 on the location of YAP. (A) IP analysis of the interaction between YAP and MDM2 proteins in HepG2 cells treated with different concentrations of CA. (B–D) CA treatment affected the intracellular localization of YAP and MDM2 proteins, as measured by the Western blotting assay. (E) Immunofluorescence technology was used to assess the subcellular location of YAP and MDM2 proteins after HepG2 cells were treated with 40 μM CA for different times. (F) Western blotting analysis of the expression of MDM2 after HepG2 cells were transfected with sh-MDM2 or sh-NC. (G) IP assay analysis of the ubiquitination of YAP after HepG2 cells were transfected with sh-MDM2 or sh-NC. (H, I) Western blotting analysis of the nuclear and cytoplasmic expression of YAP in HepG2 cells treated with 40 μM CA for different times together with sh-MDM2 or sh-NC.

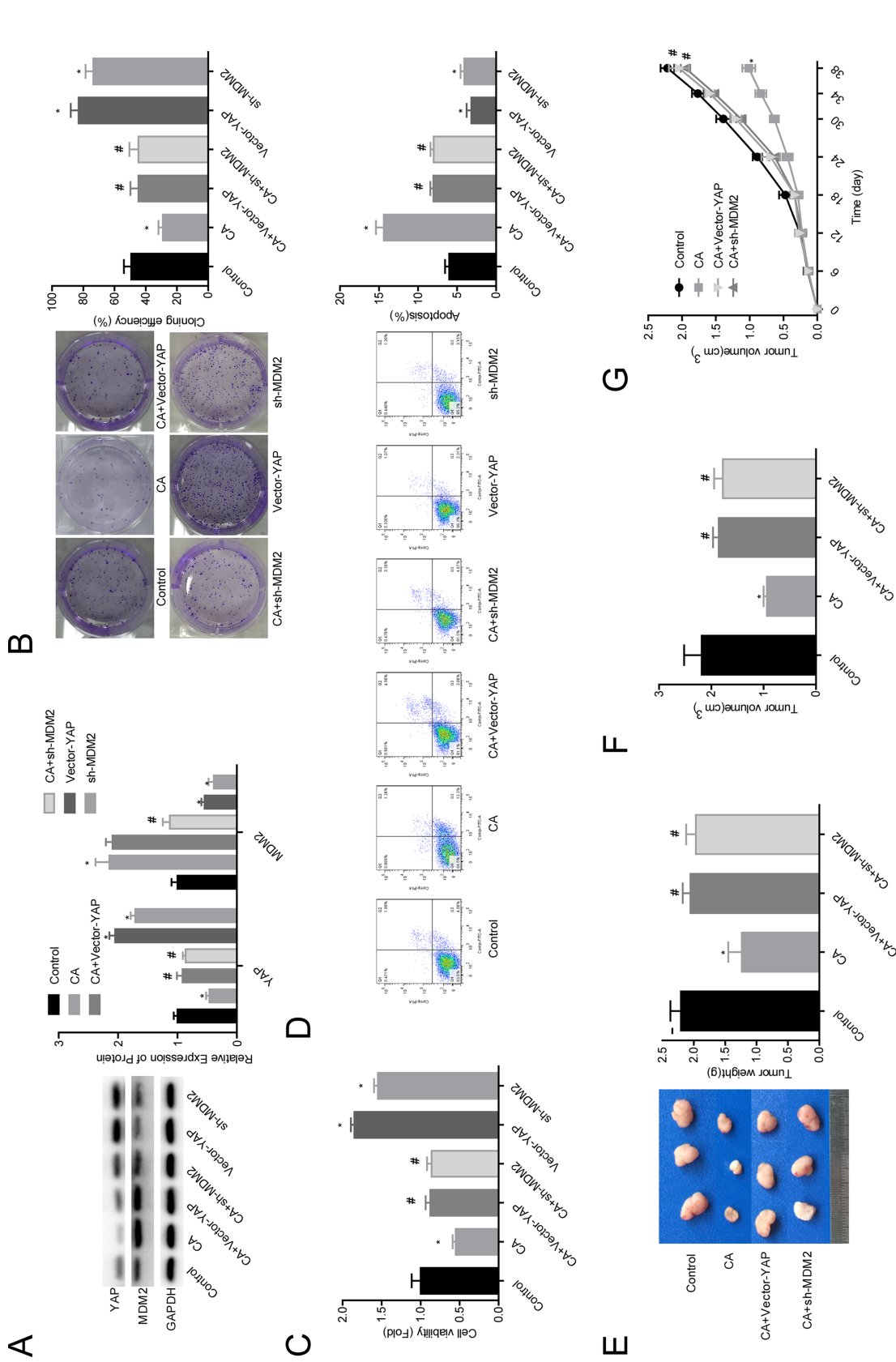


Figure 6. YAP upregulation or MDM2 downregulation abolished the role of CA in hepatocellular carcinoma (HCC) cell viability, apoptosis, and tumorigenesis. (A) The expression levels of MDM2 and YAP were determined by Western blotting analysis. (B) Cell colony formation assay was used to detect cell colony formation ability in different groups of HepG2 cells (control, CA, CA + vector-YAP, CA + sh-MDM2, vector-YAP, and sh-MDM2 groups). (C) MTT assay was performed to assess cell proliferation in different groups of HepG2 cells (control, CA, CA + vector-YAP, CA + sh-MDM2, vector-YAP, and sh-MDM2 groups). (D) Flow cytometry assay was used to test cell apoptosis. (E, F) In vivo tumor formation assay was applied to assess the effects of the MDM2/YAP axis on CA-induced tumorigenesis in HCC. (G) The tumor growth curves in different groups of mice. * $p < 0.05$, compared with control group; # $p < 0.05$, compared with CA group.

model. Similarly, the present study also demonstrated the antitumor role of CA in HCC, which inhibited cell proliferation and tumorigenesis and promoted cell apoptosis through translocating YAP from the nucleus to the cytoplasm. These results indicate that CA could be a potential chemotherapeutic agent for HCC therapy.

CA is a ursane-type triterpenoid that inhibits STAT3 in macrophages, myeloid cells, and ovarian cancer cells^{23,24}. CA also significantly inhibits endothelial angiogenic tube formation²⁵ and tumor growth in lung²⁶, ovarian²⁴, and liver cancer cells¹¹. We also observed that CA had an anticancer effect in SMMC-7721, Hep3B, HepG2, Huh7, and HLE cells. CA at concentrations between 0 and 10 μM was not cytotoxic to cells, and the IC_{50} of CA was about 40 μM . CA was reported to play an antitumor role largely due to its promotion of apoptosis, which inhibited cell viability in both a dose- and a time-dependent manner and triggered the activation of caspase 8, caspase 9, and caspase 3 in human cervix adenocarcinoma HeLa cells²⁷. Therefore, we focused on apoptosis in the present study. Our results were consistent with these findings and demonstrated that CA significantly inhibited cell proliferation and promoted cell apoptosis in SMMC-7721, Hep3B, HepG2, Huh7, and HLE cells in a dose-dependent manner.

YAP, a transcriptional coactivator of the Hippo pathway, plays an important role in regulating cell proliferation and organ development²⁸. The function of YAP is associated with a series of transcription factors including the TEAD family, and their interactions activate the transcription of genes such as Runx2 and CREB that control transformative phenotypes in cancer cells^{29,30}. The TEAD–YAP complex not only is frequently hyperactive in breast cancer but also exhibits strong oncogenic activity in liver cancer³¹. YAP can also associate with Runx2 and control downstream Runx2 signaling cascades^{32,33}. Additionally, Wang et al.¹⁸ reported that the YAP–CREB interaction was critical for liver cancer cell survival and the maintenance of transformative phenotypes both in vitro and in vivo. Both CREB and YAP are highly expressed in a subset of human liver cancer samples and are closely correlated. CREB promotes YAP transcriptional output through binding to –608/–439, a novel region in the YAP promoter. In contrast, YAP promotes the stabilization of CREB through its interaction with mitogen-activated protein kinase 14 (MAPK14/p38) and beta-transducin repeat-containing E3 ubiquitin protein ligase (BTRC). Here we observed that CA decreased YAP stability through accelerating its ubiquitination and reducing the binding of YAP with CREB, TEAD, and Runx2. CA treatment reduced the binding of YAP to TEAD, possibly because CA translocated YAP from the nucleus to the cytoplasm.

It is well documented that the YAP-induced promotion of cell proliferation and survival is determined by its

nuclear translocation^{15,34}. Our study demonstrated that CA could translocate YAP from the nucleus to the cytoplasm, which explains the inhibition of proliferation and promotion of apoptosis by CA. Moreover, the current study demonstrated that CA translocated MDM2 from the nucleus to the cytoplasm before YAP. MDM2 was originally identified as a gene that was overexpressed in a spontaneously transformed mouse cell line (3T3-DM)³⁵, and its gene product was found to transform normal cells³⁶. MDM2 overexpression is clinically correlated with metastasis, drug resistance, and the poor prognosis of liver cancer^{37–39}. However, the present study demonstrated that the upregulation of MDM2 reduced the expression of CREB, TEAD, and Runx2 and their binding with YAP as well as the decreased expression of the transcriptional regulators ankyrin repeat domain 1 (ANKRD1) and CTGF. CTGF⁴⁰, cyclin D1⁴¹, and ANKRD1⁴² are target genes of YAP that promote its induction of growth. ANKRD1 played an antiapoptotic role in mice cardiomyocytes by inducing the expression of Bax⁴³.

As MDM2 is an E3 ubiquitin ligase, we speculated that CA promoted the ubiquitination of YAP through promoting its combination with MDM2 and accelerating the degradation of YAP. As expected, the IP assay showed that the ubiquitination level of YAP protein was significantly decreased when MDM2 was downregulated in HCC cells. In addition, the downregulation of MDM2 impaired the translocation of YAP from the nucleus and increased the tumorigenesis of HepG2 cells under CA administration, suggesting that CA-induced YAP translocation from the nucleus and tumorigenesis inhibition require the presence of MDM2. Moreover, it has been reported that there are interactions between p53 and YAP. The wild-type p53 is usually associated with the suppression of YAP oncogenic activity, while mutant p53 differently interacts with YAP⁴⁴. MDM2 is established to inhibit tumor suppressor p53⁴⁵, suggesting that MDM2 might play an oncogenic role via downregulating p53 expression. In the current study, we detected the effects of CA treatment on the expression of p53, and the results showed that CA treatment had no significant influence in the expression level of p53 protein in HepG2, Huh7, and p53-null Hep3B cells. However, CA treatment can positively regulate MDM2 expression. Therefore, we conjecture that CA treatment can directly downregulate YAP expression via regulating MDM2-mediated ubiquitination in a p53-independent manner.

In conclusion, the present study explored the roles and underlying mechanisms of CA in the treatment of HCC. We revealed that CA decreased cell viability and tumorigenesis and promoted cell apoptosis through translocating YAP from the nucleus in HCC in the presence of MDM2.

ACKNOWLEDGMENTS: This study was funded by the National Natural Fund (No. 81371849 and No. 81601748). Ming Jia and Yulin Xiong did most of the experiments and were

major contributors in the writing of the manuscript; Maoshi Li did parts of the experiments and analyzed the data of this study; and Qing Mao provided the idea of this study and revised the manuscript. All authors read and approved the final manuscript. The authors declare no conflicts of interest.

REFERENCES

- Singh S, Singh PP, Roberts LR, Sanchez W. Chemopreventive strategies in hepatocellular carcinoma. *Nat Rev Gastroenterol Hepatol*. 2014;11:45–54.
- Gomaa AI, Waked I. Recent advances in multidisciplinary management of hepatocellular carcinoma. *World J Hepatol*. 2015;7:673–87.
- Lord R, Suddle A, Ross PJ. Emerging strategies in the treatment of advanced hepatocellular carcinoma: The role of targeted therapies. *Int J Clin Pract*. 2011;65:182–8.
- Zender L, Spector MS, Xue W, Flemming P, Cordon-Cardo C, Silke J, Fan ST, Luk JM, Wigler M, Hannon GJ, Mu D, Lucito R, Powers S, Lowe SW. Identification and validation of oncogenes in liver cancer using an integrative oncogenomic approach. *Cell* 2006;125:1253–67.
- Mlynarsky L, Menachem Y, Shibolet O. Treatment of hepatocellular carcinoma: Steps forward but still a long way to go. *World J Hepatol*. 2015;7:566–74.
- Lu B, Hu M, Liu K, Peng J. Cytotoxicity of berberine on human cervical carcinoma HeLa cells through mitochondria, death receptor and MAPK pathways, and in-silico drug-target prediction. *Toxicol In Vitro* 2010;24:1482–90.
- Zhai XF, Chen Z, Li B, Shen F, Fan J, Zhou WP, Yang YK, Xu J, Qin X, Li LQ, Ling CQ. Traditional herbal medicine in preventing recurrence after resection of small hepatocellular carcinoma: A multicenter randomized controlled trial. *J Integr Med*. 2013;11:90–100.
- Ling CQ, Yue XQ, Ling C. Three advantages of using traditional Chinese medicine to prevent and treat tumor. *J Integr Med*. 2014;12:331–5.
- Yang N, Han F, Cui H, Huang J, Wang T, Zhou Y, Zhou J. Matrine suppresses proliferation and induces apoptosis in human cholangiocarcinoma cells through suppression of JAK2/STAT3 signaling. *Pharmacol Rep*. 2015;67:388–93.
- Zheng GY, Xin HL, Li B, Xu YF, Yi TJ, Ling CQ. Total saponin from root of *Actinidia valvata* Dunn prevents the metastasis of human hepatocellular carcinoma cells. *Chin J Integr Med*. 2012;18:197–202.
- Ku CY, Wang YR, Lin HY, Lu SC, Lin JY. Corosolic acid inhibits hepatocellular carcinoma cell migration by targeting the VEGFR2/Src/FAK pathway. *PLoS One* 2015;10:e0126725.
- Cong X, Lu C, Huang X, Yang D, Cui X, Cai J, Lv L, He S, Zhang Y, Ni R. Increased expression of glycinamide ribonucleotide transformylase is associated with a poor prognosis in hepatocellular carcinoma, and it promotes liver cancer cell proliferation. *Hum Pathol*. 2014;45:1370–8.
- Zhuang PY, Zhang KW, Wang JD, Zhou XP, Liu YB, Quan ZW, Shen J. Effect of TALEN-mediated IL-6 knockout on cell proliferation, apoptosis, invasion and anti-cancer therapy in hepatocellular carcinoma (HCC-LM3) cells. *Oncotarget* 2017;8:77915–27.
- Edgar BA. From cell structure to transcription: Hippo forges a new path. *Cell* 2006;124:267–73.
- Harvey K, Tapon N. The Salvador–Warts–Hippo pathway—An emerging tumour-suppressor network. *Nat Rev Cancer* 2007;7:182–91.
- Pan D. The hippo signaling pathway in development and cancer. *Dev Cell* 2010;19:491–505.
- Oudhoff MJ, Braam MJS, Freeman SA, Wong D, Rattray DG, Wang J, Antignano F, Snyder K, Refaeli I, Hughes MR, McNagny KM, Gold MR, Arrowsmith CH, Sato T, Rossi FMV, Tatlock JH, Owen DR, Brown PJ, Zaph C. SETD7 controls intestinal regeneration and tumorigenesis by regulating Wnt/beta-catenin and Hippo/YAP signaling. *Dev Cell* 2016;37:47–57.
- Wang J, Ma L, Weng W, Qiao Y, Zhang Y, He J, Wang H, Xiao W, Li L, Chu Q, Pan Q, Yu Y, Sun F. Mutual interaction between YAP and CREB promotes tumorigenesis in liver cancer. *Hepatology* 2013;58:1011–20.
- Tang X, Chen X, Xu Y, Qiao Y, Zhang X, Wang Y, Guan Y, Sun F, Wang J. CD166 positively regulates MCAM via inhibition to ubiquitin E3 ligases Smurf1 and betaTrCP through PI3K/AKT and c-Raf/MEK/ERK signaling in Bel-7402 hepatocellular carcinoma cells. *Cell Signal*. 2015;27:1694–702.
- Qiao Y, Zhang X, Zhang Y, Wang Y, Xu Y, Liu X, Sun F, Wang J. High glucose stimulates tumorigenesis in hepatocellular carcinoma cells through AGER-dependent O-GlcNAcylation of c-Jun. *Diabetes* 2016;65:619–32.
- Mommer L, Wagemaker CA, H DEK, Ouborg NJ. Unravelling below-ground plant distributions: A real-time polymerase chain reaction method for quantifying species proportions in mixed root samples. *Mol Ecol Resour*. 2008;8:947–53.
- Zhang B, Gong A, Shi H, Bie Q, Liang Z, Wu P, Mao F, Qian H, Xu W. Identification of a novel YAP-14-3-3zeta negative feedback loop in gastric cancer. *Oncotarget* 2017;8:71894–910.
- Fujiwara Y, Takeya M, Komohara Y. A novel strategy for inducing the antitumor effects of triterpenoid compounds: Blocking the protumoral functions of tumor-associated macrophages via STAT3 inhibition. *Biomed Res Int*. 2014;2014:348539.
- Fujiwara Y, Takaishi K, Nakao J, Ikeda T, Katabuchi H, Takeya M, Komohara Y. Corosolic acid enhances the antitumor effects of chemotherapy on epithelial ovarian cancer by inhibiting signal transducer and activator of transcription 3 signaling. *Oncol Lett*. 2013;6:1619–23.
- Zhu WJ, Yu DH, Zhao M, Lin MG, Lu Q, Wang QW, Guan YY, Li GX, Luan X, Yang YF, Qin XM, Fang C, Yang GH, Chen HZ. Antiangiogenic triterpenes isolated from Chinese herbal medicine *Actinidia chinensis* Planch. *Anticancer Agents Med Chem*. 2013;13:195–8.
- Horlad H, Fujiwara Y, Takemura K, Ohnishi K, Ikeda T, Tsukamoto H, Mizuta H, Nishimura Y, Takeya M, Komohara Y. Corosolic acid impairs tumor development and lung metastasis by inhibiting the immunosuppressive activity of myeloid-derived suppressor cells. *Mol Nutr Food Res*. 2013;57:1046–54.
- Xu Y, Ge R, Du J, Xin H, Yi T, Sheng J, Wang Y, Ling C. Corosolic acid induces apoptosis through mitochondrial pathway and caspase activation in human cervix adenocarcinoma HeLa cells. *Cancer Lett*. 2009;284:229–37.
- Piccolo S, Dupont S, Cordenonsi M. The biology of YAP/TAZ: Hippo signaling and beyond. *Physiol Rev*. 2014;94:1287–312.
- Pobbati AV, Han X, Hung AW, Weiguang S, Huda N, Chen GY, Kang C, Chia CS, Luo X, Hong W, Poulsen A. Targeting the central pocket in human transcription factor TEAD as a potential cancer therapeutic strategy. *Structure* 2015;23:2076–86.

30. Qiao Y, Lin SJ, Chen Y, Voon DC, Zhu F, Chuang LS, Wang T, Tan P, Lee SC, Yeoh KG, Sudol M, Ito Y. RUNX3 is a novel negative regulator of oncogenic TEAD-YAP complex in gastric cancer. *Oncogene* 2016;35:2664–74.
31. Cai WY, Lin LY, Hao H, Zhang SM, Ma F, Hong XX, Zhang H, Liu QF, Ye GD, Sun GB, Liu YJ, Li SN, Xie YY, Cai JC, Li BA. Yes-associated protein/TEA domain family member and hepatocyte nuclear factor 4-alpha (HNF4alpha) repress reciprocally to regulate hepatocarcinogenesis in rats and mice. *Hepatology* 2017; 65:1206–21.
32. Hong JH, Hwang ES, McManus MT, Amsterdam A, Tian Y, Kalmukova R, Mueller E, Benjamin T, Spiegelman BM, Sharp PA, Hopkins N, Yaffe MB. TAZ, a transcriptional modulator of mesenchymal stem cell differentiation. *Science* 2005;309:1074–8.
33. Zaidi SK, Sullivan AJ, Medina R, Ito Y, van Wijnen AJ, Stein JL, Lian JB, Stein GS. Tyrosine phosphorylation controls Runx2-mediated subnuclear targeting of YAP to repress transcription. *EMBO J.* 2004;23:790–9.
34. Mao Y, Chen X, Xu M, Fujita K, Motoki K, Sasabe T, Homma H, Murata M, Tagawa K, Tamura T, Kaye J, Finkbeiner S, Blandino G, Sudol M, Okazawa H. Targeting TEAD/YAP-transcription-dependent necrosis, TRIAD, ameliorates Huntington's disease pathology. *Hum Mol Genet.* 2016;25:4749–70.
35. Cahilly-Snyder L, Yang-Feng T, Francke U, George DL. Molecular analysis and chromosomal mapping of amplified genes isolated from a transformed mouse 3T3 cell line. *Somat Cell Mol Genet.* 1987;13:235–44.
36. Fakhrazadeh SS, Trusko SP, George DL. Tumorigenic potential associated with enhanced expression of a gene that is amplified in a mouse tumor cell line. *EMBO J.* 1991;10:1565–9.
37. Zhu MH, Ni CR, Zhu Z, Li FM, Zhang SM. [Determination of expression of eight p53-related genes in hepatocellular carcinoma with tissue microarrays]. *Ai Zheng* 2003;22:680–5.
38. Zhou XD. Recurrence and metastasis of hepatocellular carcinoma: Progress and prospects. *Hepatobiliary Pancreat Dis Int.* 2002;1:35–41.
39. Ranjan A, Bera K, Iwakuma T. Murine double minute 2, a potential p53-independent regulator of liver cancer metastasis. *Hepatoma Res.* 2016;2:114–21.
40. Zhao B, Ye X, Yu J, Li L, Li W, Li S, Lin JD, Wang CY, Chinnaiyan AM, Lai ZC, Guan KL. TEAD mediates YAP-dependent gene induction and growth control. *Genes Dev.* 2008;22:1962–71.
41. Mizuno T, Murakami H, Fujii M, Ishiguro F, Tanaka I, Kondo Y, Akatsuka S, Toyokuni S, Yokoi K, Osada H, Sekido Y. YAP induces malignant mesothelioma cell proliferation by upregulating transcription of cell cycle-promoting genes. *Oncogene* 2012;31:5117–22.
42. Stein C, Bardet AF, Roma G, Bergling S, Clay I, Ruchti A, Agarinis C, Schmelzle T, Bouwmeester T, Schubeler D, Bauer A. YAP1 exerts its transcriptional control via TEAD-mediated activation of enhancers. *PLoS Genet* 2015;11:e1005465.
43. Shen L, Chen C, Wei X, Li X, Luo G, Zhang J, Bin J, Huang X, Cao S, Li G, Liao Y. Overexpression of ankyrin repeat domain 1 enhances cardiomyocyte apoptosis by promoting p53 activation and mitochondrial dysfunction in rodents. *Clin Sci. (Lond)* 2015;128:665–78.
44. Cui M, Li Z. Downregulation of YAP inhibits proliferation and induces apoptosis in Eca-109 cells. *Exp Ther Med.* 2018;15:1048–52.
45. Nag S, Zhang X, Srivenugopal KS, Wang MH, Wang W, Zhang R. Targeting MDM2-p53 interaction for cancer therapy: Are we there yet? *Curr Med Chem.* 2014;21:553–74.